X-ray Photoelectron Spectroscopy Study of Interactions Between Gold Nanoparticles and Epidermal Growth Factor…

Article *in* Journal of Bionanoscience · April 2017

DOI: 10.1166/jbns.2017.1420

CITATIONS
0

READS
23

7 authors, including:

Victor Sanchez-Mendieta
Universidad Autónoma del Estado de México …
60 PUBLICATIONS **653** CITATIONS
SEE PROFILE

Liliana Argueta-Figueroa
Escuela Nacional de Estudios Superiores (EN…
12 PUBLICATIONS **104** CITATIONS
SEE PROFILE

Raul Alberto Morales Luckie
Universidad Autónoma del Estado de México …
39 PUBLICATIONS **174** CITATIONS
SEE PROFILE

Journal of
Bionanoscience
Vol. 11, 1–7, 2017

Study X-ray Photoelectron Spectroscopy Determination of Interactions Between Gold Nanoparticles and Epidermal Growth Factor for Potential Use in Biomedicine

María G. González-Pedroza[1], Víctor Sánchez-Mendieta[1], Jorge A. Morales-Valencia[2,4], Gustavo López-Téllez[1], Liliana Argueta-Figueroa[3], Oscar González-Pérez[4], and Raúl A. Morales-Luckie[1,*]

[1] *Centro Conjunto de Investigación en Química Sustentable UAEMex-UNAM (CCIQS), 50200, Toluca, Estado de México, México*
[2] *Instituto Tecnológico y de Estudios Superiores de Monterrey (ITESM)*
[3] *Laboratorio de Investigación Interdisciplinaria, Nanoestructuras y Biomateriales, Escuela Nacional de Estudios Superiores (ENES) Unidad León, Universidad Nacional Autónoma de México (UNAM)*
[4] *Laboratrorio de Neurociencias, Facultad de Psicología, Universidad de Colima, Colima 28040, México*

Nowadays, biomedical applications of gold nanoparticles coupled with Epidermal Growth Factor have attracted huge attention because of its theranostic activity, which could be useful for diagnosis and treatment of neurodegenerative diseases. Therefore, there is a great interest to know the nature of the intermolecular interactions between the gold nanoparticles and epidermal growth factor (EGF). A two-step synthesis was performed. In the first step, gold nanoparticles were synthesized by chemical reduction of tetrachloroauric acid using sodium citrate as reducing and capping agent. Secondly, gold nanoparticles were coupled with EGF. The obtained nanoparticles were characterized by ultraviolet-visible spectroscopy, transmission electron microscopy, X-ray photoelectron spectroscopy and zeta-potential before and after being coupled with the EGF. Gold nanoparticles with an average diameter of 8.09 nm were obtained. After coupled with EGF, the particle average diameter increased to 9.14 nm. X-ray photoelectron spectroscopy showed an electrostatic interaction between gold nanoparticles and EGF. Zeta potential corroborated these results. Thus, it was possible for the first time to identify the interactions between these two chemical species. Since gold nanoparticles may act as carriers of EGF, these results illustrate the great potential for the use of this bionanocomposite in neurodegenerative disease treatment.

Keywords: Electrostatic Interactions, Coupling Gold Nanoparticles, Epidermal Growth Factor, Neurodegenerative Disease, Bionanocomposite.

RESEARCH ARTICLE

1. INTRODUCTION

Biomedical applications of nanotechnology include delivery of drugs;[1,2] detection of molecules, organisms and viruses;[3] controlled drugs targeting; diagnosis by magnetic resonance imaging;[4] treatment of neurodegenerative diseases such as cancer, diabetes mellitus, among others.[5] The epidermal growth factor (EGF) is involved in various stages of cell proliferation, tissue regeneration, cell survival and more.[6] Recent studies support the hypothesis that low EGF levels detected in cerebrospinal fluid of patients with multiple sclerosis diagnose may be causally related to the disease.[7,8] In fact, EGF strongly promotes the proliferation and migration of oligodendrocytes (the major function of these cells is the formation of myelin), in both, physiological and pathological conditions.[9,10] Therefore, it has been suggested that myelin-related to EGF may improve the remyelination process in multiple sclerosis or other demyelinating diseases.[11]

EGF possesses three disulfide bridges, peptide bonds and a free amino α group at the beginning of the chain. Besides, EGF has an arginine carboxy group in their β form; it is heat stable and is inactivated at 40 °C.[12] The protein structure of the EGF is shown in Figure 1.

Gold nanoparticles (AuNPs) have physical, chemical and biological properties that are related to their size and morphology; the understanding of these tailoring properties is essential for the AuNPs applications.[13] Recently, one of the most common methods of NPs synthesis is the chemical reduction of a gold precursor salt using sodium citrate as reducing and capping agent. Turkevich, in 1951, reported the basic experimental approach

*Author to whom correspondence should be addressed.

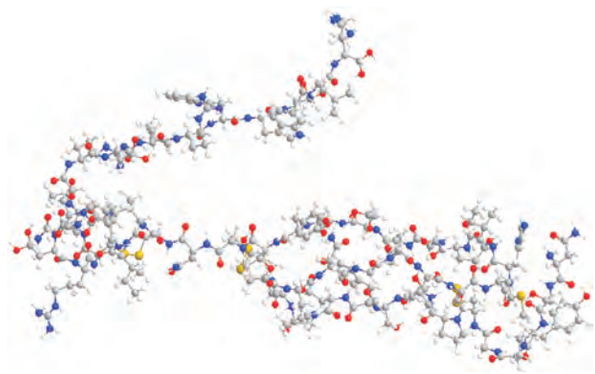

Fig. 1. Epidermal growth factor (EGF) representation.

to produce AuNPs and described the effect of temperature and sodium citrate concentration on the size of nanoparticles. These nanoparticles can be easily functionalized with a wide range of ligands (antibodies, polymers, diagnostic probes, drugs, genetic material, etc.).[14–16]

Hybrid nanoparticles (with organic and inorganic parts) have emerged as a simple solution for the generation of theranostic systems.[17] Thus, the design of this type of nanoparticles has been an important source of such systems.[16] In addition, the frequency of plasmon surface resonance of the gold nanoparticles is closely related to system properties such as size, shape, miscibility, binder, dielectric properties, surface functionalization and the refractive index of the surrounding medium.[18]

Today, there are numerous studies on conjugation of molecules like EGF to metallic nanoparticles (Au, Pt, Ag, Fe_2O_3). The EGF delivery is a beneficial method for chronic degenerative diseases diagnosis and treatment in terms of targeted therapy.[19] Due to this, the nanoparticles have a high surface area to volume-ratio.[20] Therefore, to determine the synthesis and chemical properties of this biocomposite is an important step to the development of AuNPs with clinical applications.[16]

A variety of chemical functional groups that could interact with the AuNPs, including imidazole, sulfur, aromatic rings, amine, and carboxylate groups, have been established in the literature. Different kinds of interactions between gold and sulfur, gold and thiols, among others, have been identified.[21, 22] Furthermore, at the nanoscale, the AuNPs also exhibit electrostatic interactions with the amine groups.[23] Whereas, the amine groups establish similar interactions with carboxyl groups present on the surface of AuNPs that have been capped with sodium citrate.[24–26]

The main aim of the present study was to synthesize AuNPs by chemical reduction of tetrachloroauric acid, using sodium citrate as reducing and capping agent, and the further coupling of the AuNPs with EGF, to determine the kind of the interactions between them.

2. MATERIALS AND METHODS

2.1. Synthesis of AuNPs

The AuNPs were synthesized using the citrate reduction method from a 1% $HAuCl_4$ colloidal suspension. Firstly, 100 ml of deionized H_2O were heated to boiling point and then, 5.0 ml of sodium citrate solution (0.05 M in 50 ml of deionized H_2O) were quickly added into the flask and stirred into solution for at least 20 min until a ruby-red color solution was obtained.[24]

2.2. Preparation of Coupling AuNPs-EGF

The AuNPs coated with EGF were prepared according to the method described by Sokolov, et al., 2006. The AuNPs were diluted in HEPES buffer solution at 20 mM (pH 7.4, Sigma-Aldrich) until a final optical density of 0.8 at 530 nm was obtained. Subsequently, 50 μl of EGF (Sigma-Aldrich) were diluted in 500 μl of the same HEPES buffer solution. Then, 10 ml of the solution previously prepared of AuNPs in colloidal solution were mixed with the diluted solution of EGF for 20 min. Afterwards, 0.5 ml of 1% polyethylene glycol (MW = 4000, Boehringer) were added to the mixture to prevent aggregation and the mixture was centrifuged at 6000 rpm for 18 min. Finally, the biocomposite (AuNPs-EGF) was redispersed in PBS buffer (pH 7.4) and stored at 4 °C.

2.3. Characterization of the AuNPs Before and After Their Coupling with EGF

The optical properties of the AuNPs before and after their coupling with EGF were determined using UV-Vis spectroscopy (Varian Cary 5000 UV-Vis-NIR, Agilent Technologies, UK). Two samples were prepared and diluted, 1 ml of AuNPs and 1 ml of biocomposite (AuNPs-EGF) in deionized water, each one for separate characterization. Then, each sample was analyzed in a range of 200–800 nm in the absorption mode. Structural properties of the nanoparticles formed, such as morphology, size and particle distribution were characterized using a Transmission Electron Microscope (TEM) (JEOL-2100 200 kV with LaB6 filament). A drop of the AuNPs and a drop of the biocomposite (AuNPs-EGF) were placed on grids and allowed to dry for 20 min before the analysis. FTIR analysis was performed (Bruker, Model 27) to investigate and characterize functional groups that are present in the EGF, to verify the presence of AuNPs in the biocomposite (AuNPs-EGF) and to elucidate the interactions between the AuNPs and the EGF. FTIR technique was carried out by placing a drop of each sample on the analysis device and operating under standard conditions.

Zeta potential measurements were determined using the Zetasizer 2000 (Malvern Instruments Ltd., Worcestershire, UK). The voltage applied to driving electrodes of the cell was 150 V of capillary electrophoresis. The sample was prepared by injecting approximately 2 ml of solution in the cell.

RESEARCH ARTICLE

To determine the interactions between the functional groups of EGF and the surface of the AuNPs, the biocomposite was analyzed by X-ray photoelectron spectroscopy (XPS). XPS spectra were acquired using a JEOL JPS-9200, equipped with an X-ray source Mg (1253.6 eV) at 300 W, the area of analysis was 3 mm^2, and vacuum was of the order of 7.5×109 Torr for all samples. The spectra were analyzed using the included software with the instrument specsurfTM in all load spectra were corrected by signal accidental carbon (C 1*s*) to 284.5 eV. The Shirley method was used for background subtraction, while the curve was used to the Gauss-Lorentz.

3. RESULTS AND DISCUSSION

3.1. Synthesis of AuNPs

The obtained AuNPs give rise to a ruby red colloidal solution. This color is attributed to the size and spherical shape of the AuNPs nanoparticles. In contrast, the Au nanorods show different colors in solution, according to the reported by El-Sayed et al.[24] More recent studies have shown that the color of the colloidal solution is due to various conditions: size, shape, crystallinity, interparticle interactions, and the collective oscillation of electrons in the conduction band, which is known as surface plasmon oscillation[27] and the dielectric constant of the surrounding medium.[28] As a result, the solvent used will have an effect on the oscillation frequency due to the varying ability of the surface to accommodate the electron charge density from the nanoparticles.[29]

3.2. Coupling of AuNPs with EGF

The coupling of AuNPs with EGF can be distinguished by a precipitate formation after the mixture is centrifuged, which from this point will be referred as the bionanocomposite. The main characteristics of this bionanocomposite are the sensitivity to changes of pH and to high temperatures; when the ambient temperature exceeds 40 °C, the EGF protein is denaturalized.[30] Therefore, the mixture must be stored at 4 °C to avoid denaturalization and maintain the pH of the solution during the coupling process though the addition of HEPES buffer solution.

3.3. UV-Vis Analysis

In the UV-Vis spectrum of the AuNPs (Fig. 2) a single peak of maximum absorption is observed at 520 nm. According to that reported by El-Sayed et al.,[24] a maximum absorbance peak at 530 nm corresponds to a gold particle size of 40 nm. Sokolov et al. 2008[31] reported a maximum absorption peak at 540 nm, obtaining AuNPs with an average particle size of 50 nm. Liz-Marzán et al.,[27] and Eustis et al.,[29] demonstrated that the number of peaks represents the morphology of nanoparticles, which means that the presence of a single peak refers to a spherical morphology. In contrast, if the spectrum shows the presence

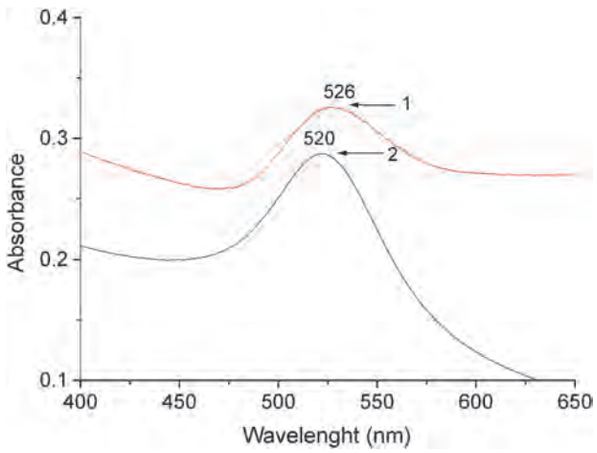

Fig. 2. UV-visible spectra; (curve 1) bionanocomposite (EGF-AuNPs), (curve 2) AuNPs.

of two absorbance bands, it means that the morphology correspond to the nanorods shape.[27] Due to the aforementioned, it is possible to assume that the morphology of the AuNPs synthesized is spherical. By analyzing the different absorption peaks previously reported, it was determined that variations depend directly on the added amount of sodium citrate and the concentration of $HAuC_4$. Due to this, the intensity of absorption in the spectrum is affected by the size of the nanoparticles. If the maximum absorption peak was observed and a red-shift of a few nanometers occurs, this indicates an increase in the size of the nanoparticles. This event is due to the collective oscillation of electrons in an electromagnetic field, since the larger the size of the nanoparticle a higher oscillation is registered as consequence.[24, 32]

In the UV-Vis spectrum of the bionanocomposite AuNPs-EGF (Fig. 1), a red-shift of 6 nm was observed in comparison to the AuNPs spectrum (Fig. 2) without EGF.[33] This shift was associated to the core obtained when the nanoparticles are functionalized with other agents, in this case, with proteins. In addition, another possible explanation for that event may be the aggregations of NPs as a result of surface modification,[34] instead of the simple change of size of the functionalized nanoparticle.

3.4. TEM Analysis

In the TEM micrographs (Fig. 3) the presence of AuNPs synthesized from sodium citrate is observed, and a spherical morphology can be seen. In addition, it was confirmed that the nanoparticles exhibit a uniform distribution without agglomerates. In the SAED (Fig. 3), the measurements of the interplanar distances correspond to the planes (111), (220) and (311) in accordance with the structure the face centered cubic of metallic gold which correspond to JCPDS file: 004-0784. In the bionanocomposite's TEM micrographs (Fig. 3), a good distribution of particle sizes is observed; besides, the AuNPs maintain their morphology

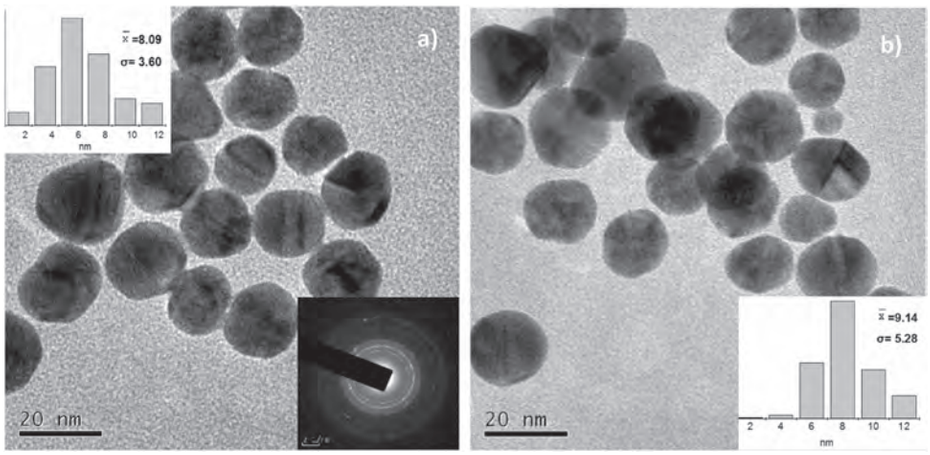

Fig. 3. TEM observations. (a) Micrograph of AuNPs (c) the X-ray diffraction pattern, (b) micrograph of binonanocomposite (EGF-AuNPs), insets show the particles size distribution.

even after coupled with EGF. The histogram (Fig. 3) shows an increase in average particle size compared to the size of the NPs obtained before coupling. The size of the AuNPs was 8.09 nm, with a standard deviation of 3.60 nm. After coupling the AuNPs with EGF, the average particle size was 9.14 nm with a standard deviation of 5.28 nm. However, this increase in size was expected by molecular coupling in the Au-EGF NPs to different substances, such as PEG, PBS, and HEPES; which ensured the stability of the bionanocomposite (AuNPs-EGF). The size of the particles obtained in our study, less than 50 nm, can provide better optical properties[35] and biocompatibility.[24, 32]

3.5. Structural Characterization of the EGF with and Without Coupling to AuNPs

Usually, a FTIR spectrum of a protein is considered as a linear sum of the spectrum of its conformational changes. There are numerous well-established correlations between many infrared spectra for certain protein structures.[36] As it is shown in Figure 4, the usual bands for a protein are found. The structure of proteins, such as EGF, is characterized by nine absorption bands in the infrared.[36, 37] These bands were assigned as follows, the band found in 3325 cm^{-1} was assigned to the characteristic vibration of NH group.[38] The bands located at 1652 cm^{-1} and 1618 cm^{-1} are associated with the amides I and II,[39] which are considered the most important bands of skeletal vibration of proteins. The amide I band (between 1700–1600 cm^{-1}) is the most sensitive of all. This band is associated with the stretching vibration of C═O group of the peptide bond. Regarding the amide II band, it is mainly associated with the vibration in the plane of the NH group (flexion) and the group CN (stretching).[40, 41] Small vibration bands are observed at 1397 cm^{-1} 1260 cm^{-1},[41] which correspond to the amides III. The vibrational bands amino groups and carboxyl groups are located in 1584 cm^{-1} and 1460 cm^{-1}, respectively. These groups are characteristic of amino acids containing the protein.[42]

As shown in Figure 4, the spectra of the bionanocomposite, the OH groups of HEPES (4-(2-hydroxyethyl)-1-piperazineethanesulfonic) are located at 3446 cm^{-1} and an intense band at 1179 cm^{-1} corresponding to the sulfonic group is observed. In addition, the second band at 1074 cm^{-1} corresponding to the vibrations of ether group C–O–C, which is the most characteristic absorption band for molecules of PEG shows a strong signal.[43] This band is also associated with the C–N vibration present in this protein.

3.6. Characterization by X-ray Photoelectron Spectroscopy (XPS) and Zeta Potential

Per the nature of the synthesis of the AuNPs, it was expected that the NPs were surrounded by a layer of sodium citrate. This is confirmed by the value of zeta potential at −30 mV for AuNPs, which effectively means

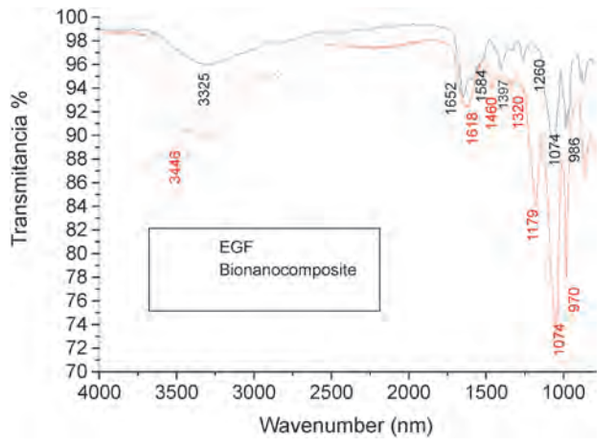

Fig. 4. FITR spectra of de protein EGF and bionanocomposite (EGF-AuNPs).

RESEARCH ARTICLE

that the nanoparticles could have a layer of citrate molecules and these molecules help to maintain the stability of the nanoparticles in aqueous solution.[44,45] When the bionanocomposite of AuNPs-EGF is synthesized, the EGF molecules, by their chemical nature, carry out two main processes for attaching to AuNPs (which are passivated with citrate). The first process involves the electrostatic interaction between the carboxylate groups from the citrate and the ammonium functional groups in EGF, or some other functional group with cationic character that could have been generated during the experimental procedure for coupling. This electrostatic interaction between biomolecules (proteins) and passivating agents (citrate molecules) of metal nanoparticles has been previously recognized by other researchers.[46,47] This first type of interaction can be associated to the value of −7 mV obtained by zeta potential for the bionanocomposite. Clearly, the magnitude of the negative charge that exists in the carboxylates of the citrate molecules surrounding the AuNPs is reduced considerably when the coupling with EGF occurs. This phenomenon is mainly due to the electrostatic interaction between carboxylates and cationic functional groups, which was generated during the coupling that, in turn, reduces the negative charge on the surface of AuNPs-EGF. Moreover, in this first interface, the EGF molecules interact, also electrostatically, with the AuNPs atoms during coupling, as reported in previous studies of coupled AuNPs with other biomolecules.[3,4] This second type of interaction or attachment can be corroborated by the peaks obtained in the XPS spectra of Au 4*f* 7/2 and of N 1*s*. To this end, AuNPs, EGF and bionanocomposite (AuNPs-EGF) samples were analyzed. In Figure 5(a), two peaks can be observed, one of them is located at 83.39 eV, corresponding to 7/2 4*f* Au0, and the other peak, located at 82.66 eV, corresponds to a satellite peak α5 of Si 2*p* 3/2 that interferes with the gold region. At the same time, it was after deconvolution in the region 4*f* 7/2 Au0 of the bionanocomposite (AuNPs-EGF) that three peaks were obtained (Fig. 5(b)). The peaks located at 83.01 eV and 83.39 eV (Fig. 5(b)) are attributed to Au0. In the spectrum of the bionanocomposite occurs a displacement of 0.38 eV of this signal compared to the same peak obtained for the AuNPs only. This displacement can be attributed to the electrostatic interaction between atoms from the AuNPs with the nitrogen from the amine groups of the EGF protein. This type of interaction has been identified by other authors.[34,48,49] The third peak is observed at 83.84 eV (Fig. 6), which may be related to a possible oxidation of the AuNPs when coupled with EGF. Some reports have attributed the emergence of new peaks at

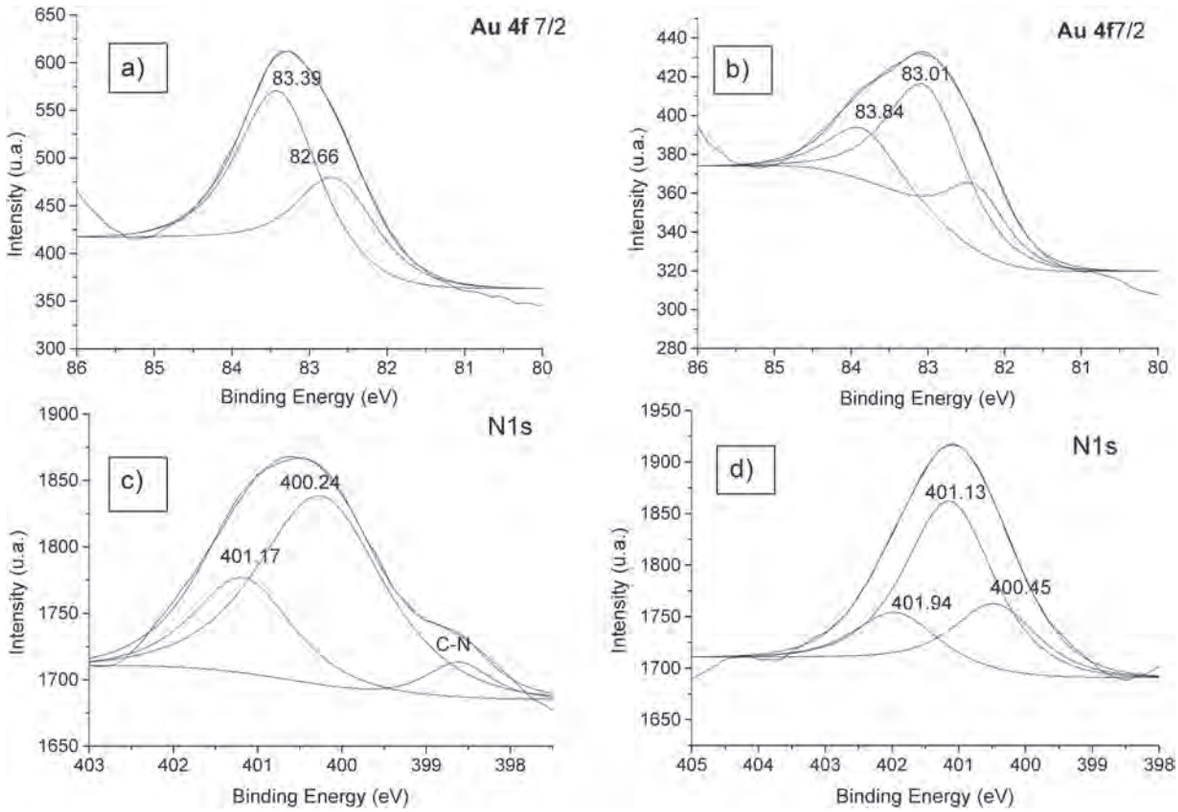

Fig. 5. XPS spectra: (a) Au 4*f* 7/2 region of AuNPs solution, (b) Au 4*f* 7/2 region of bionanocomposite (AuNPs-EGF), (c) N 1*s* region of EGF protein, (d) N 1*s* region of Bionanocomposite (AuNPs-EGF).

RESEARCH ARTICLE

higher binding energy to an oxidative reaction when gold is functionalized.[48]

Currently, a variety of functional groups that could interact with the AuNPs are known, including imidazole, sulfur, aromatic rings, amine and carboxylates.[50] In our study, we recognized the presence of zwitterions in EGF molecule located at a terminal end of the protein chain and formed by five basic amino acids. This protein possesses four amino acids of ARG (arginine) and one amino acid of HIS (histidine),[51] as is shown in Figure 1.

In order to further demonstrate the interaction occurring between Au and nitrogen moieties present in EGF, the N 1*s* region of XPS spectrum was deconvoluted. The spectrum in the N 1*s* region corresponding to EGF is shown in Figure 21(c), the peak located at 400.24 eV is consistent with the binding energy of the amine group.[38] The second peak with lower intensity at 401.17 eV is associated with the binding energy of protonated amines. In the XPS spectrum of the bionanocomposite (AuNPs-EGF) as illustrated in Figure 21(d), there is a shift of this last signal (0.38 eV), which can be attributed to the electrostatic interaction between the nitrogen atoms of protonated amines of the protein with the AuNPs. This type of interaction is in concordance with the ones proposed by other authors.[22, 34, 49, 52] Furthermore, similar energy changes have been observed when the AuNPs system is functionalized, indicating a physical absorption.[49, 53]

Other studies described that due to the AuNPs coupling with other proteins.[22] So, extra peaks appear with lower intensity but higher binding energy, they provide an increase of 0.8 eV.[22] In our system, the binding energy was 0.77 eV, which is consistent with previous findings of interactions between metallic nanoparticles and biomolecules. This event excludes the possibility of interactions with thiol groups because the sulfur found between the cysteinemolecules forms disulfide bridges. Methionine is another amino acid that could interact with AuNPs. However, there is only one of methionine amino acid in the EGF structure. Despite this, these amino acids are not exposed on the surface of the EGF moiety; therefore these amino acids are not accessible binding sites to interact with the AuNPs.[22, 54] According to the current results, both zeta potential (surface charge variations) and XPS analysis (displacement of binding energies) determine that the coupling of AuNPs (passivated with citrate) with the EGF occurs mainly as electrostatic interactions.

One of the biggest advantages of using AuNPs coupled to biomolecules is their excellent biocompatibility,[56] due to the weak interactions that AuNPs have with some proteins and amino acids *in vivo*.[55, 56] A high percentage of these AuNPs is cleared by the mononuclear phagocyte system (macrophages),[57, 58] and only a low amount of AuNPs (about 3%) is accumulated in the liver and very high concentrations are required to produce hepatotoxicity.[48] Due to the binding of the EGF is electrostatic, the use of AuNPs as drug carriers is promising. Hence, the bionanocomposite AuNPs-EGF has a great potential to use for treatment in diseases where EGF could act as treatment, for example, in multiple sclerosis or demyelinating diseases. However, further studies *in vivo* are required to determine other biological aspects, such as biodistribution, dosing and possible side effects in the organism.

4. CONCLUSIONS

AuNPs with a less than 10 nm diameter were synthesized by the citrate method and coupled successfully to the EGF. The bionanocomposite (AuNPs-EGF) was satisfactorily characterized ultraviolet-visible spectroscopy, infrared spectroscopy, transmission electron microscopy, X-ray photoelectron spectroscopy and zeta-potential. The main interactions of the AuNPs and the cationic moieties in the EGF protein were identified as electrostatic in nature by means of X-ray photoelectron spectroscopy (XPS).

Conflict of Interest

The authors declare no conflict of interest.

Acknowledgments: This work was supported by grants kindly provided by ConsejoNacional de Ciencia y Tecnologia (No. 2015-01-465) and UAEMex (3789/2014/CIA).

References and Notes

1. B. Senthilkumar and R. Rajasekaran, *J. Bionanosci.* 10, 1 (**2016**).
2. E. E. Connor, J. Mwamuka, A. Gole, C. J. Murphy, and M. D. Wyatt, *Small* 1, 325 (**2005**).
3. M. Mahmoudi, P. Stroeve, A. S. Milani, and A. S. Arbab, Superparamagnetic Iron Oxide Nanoparticles, Nova Science Publishers, Inc. (**2011**).
4. S. Y. Nam, L. M. Ricles, L. J. Suggs, and S. Y. Emelianov, *PLoS One* 7, e37267 (**2012**).
5. N. Ahmed, H. Fessi, and A. Elaissari, *Drug Discovery Today* 17, 928 (**2012**).
6. P. Erfani, J. Tome-Garcia, P. Canoll, F. Doetsch, and N. M. Tsankova, *Epigenetics* 10, 496 (**2015**).
7. M. Tejera-Alhambra, A. Casrouge, C. de Andrés, A. Seyfferth, R. Ramos-Medina, B. Alonso, J. Vega, L. Fernández-Paredes, M. L. Albert, and S. Sánchez-Ramón, *PLoS One* 10, e0128952 (**2015**).
8. A. J. Bieber, K. Suwansrinon, J. Kerkvliet, W. Zhang, L. R. Pease, and M. Rodriguez, Allelic variation in the Tyk2 and EGF genes as potential genetic determinants of CNS repair, *Proceedings of the National Academy of Sciences* (**2010**), Vol. 107, pp. 792–797.
9. L. A. Swayne and L. Wicki-Stordeur, *Channels* 6, 69 (**2012**).
10. O. Gonzalez-Perez and A. Alvarez-Buylla, *Brain Res. Rev.* 67, 147 (**2011**).
11. J. E. Caussa and E. H. Vila, *Clinical Medicine* 145, 305 (**2015**).
12. A. J. Mieszawska, W. J. Mulder, Z. A. Fayad, and D. P. Cormode, *Molecular Pharmaceutics* 10, 831 (**2013**).
13. K. Sokolov, M. Follen, J. Aaron, I. Pavlova, A. Malpica, R. Lotan, and R. Richards-Kortum, *Cancer Res.* 63, 1999 (**2003**).
14. S. Al-Qadi and C. R. López, Metal Nanoparticles: Gold, Monographs of the Royal National Academy of Pharmacy (**2009**).
15. J. Turkevich, P. C. Stevenson, and J. Hillier, *Discussions of the Faraday Society* 11, 55 (**1951**).

RESEARCH ARTICLE

16. J. Gautier, E. Allard-Vannier, E. Munnier, M. Soucé, and I. Chourpa, *J. Controlled Release* 169, 48 **(2013)**.
17. G. Sekar, A. Sivakumar, A. Mukherjee, and N. Chandrasekaran, *J. Bionanosci.* 10, 94 **(2016)**.
18. P. Sharma, S. Brown, G. Walter, S. Santra, and B. Moudgil, *Adv. Colloid Interface Sci.* 123, 471 **(2006)**.
19. Y. Chen, J. Wang, J. Wang, L. Wang, X. Tan, K. Tu, X. Tong, and L. Qi, *J. Biomed. Nanotechnol.* 12, 656 **(2016)**.
20. L. Tutkun, E. Gunaydin, M. Turk, and T. Kutsal, *J. Nanosci. Nanotechnol.* 17, 1681 **(2017)**.
21. L. Caprile, A. Cossaro, E. Falletta, C. D. Pina, O. Cavalleri, R. Rolandi, S. Terreni, R. Ferrando, M. Rossi, and L. Floreano, *Nanoscale* 4, 7727 **(2012)**.
22. J. C. Zhou, X. Wang, M. Xue, Z. Xu, T. Hamasaki, Y. Yang, K. Wang, and B. Dunn, *Mater. Sci. Eng.: C* 30, 20 **(2010)**.
23. L. Jiang and L. Gao, *Carbon* 41, 2923 **(2003)**.
24. I. H. El-Sayed, X. Huang, and M. A. El-Sayed, *Cancer Letters* 239, 129 **(2006)**.
25. A. V. Ellis, K. Vijayamohanan, R. Goswami, N. Chakrapani, L. Ramanathan, P. M. Ajayan, and G. Ramanath, *Nano Lett.* 3, 279 **(2003)**.
26. A. Eitan, K. Jiang, D. Dukes, R. Andrews, and L. S. Schadler, *Chem. Mater.* 15, 3198 **(2003)**.
27. L. M. Liz-Marzán, *Mater. Today* 7, 26 **(2004)**.
28. S. K. Ghosh and T. Pal, *Chem. Rev.* 107, 4797 **(2007)**.
29. S. Eustis and M. A. El-Sayed, *Chem. Soc. Rev.* 35, 209 **(2006)**.
30. J. O'connell and P. Fox, Advanced Dairy Chemistry—1 Proteins, Springer **(2003)**, pp. 879–945.
31. P. K. Jain, X. Huang, I. H. El-Sayed, and M. A. El-Sayed, *Acc. Chem. Res.* 41, 1578 **(2008)**.
32. X. Liu, Y. Yang, L. Mao, Z. Li, C. Zhou, X. Liu, S. Zheng, and Y. Hu, *Sensors and Actuators B: Chemical* 218, 1 **(2015)**.
33. S. J. Beebe, P. F. Blackmore, J. White, R. P. Joshi, and K. H. Schoenbach, *Physiological Measurement* 25, 1077 **(2004)**.
34. H. Joshi, P. S. Shirude, V. Bansal, K. Ganesh, and M. Sastry, *The Journal of Physical Chemistry B* 108, 11535 **(2004)**.
35. M. Auffan, J. Rose, J.-Y. Bottero, G. V. Lowry, J.-P. Jolivet, and M. R. Wiesner, *Nat. Nanotechnol.* 4, 634 **(2009)**.
36. J. Kong and S. Yu, *Acta Biochimica et Biophysica Sinica* 39, 549 **(2007)**.
37. A. Adochitei and G. Drochioiu, *Rev. Roum. Chim.* 56, 783 **(2011)**.
38. Z. Ren, X. Xu, X. Wang, B. Gao, Q. Yue, W. Song, L. Zhang, and H. Wang, *J. Colloid Interface Sci.* 468, 313 **(2016)**.
39. Z. Sun, H. Xu, Y. Cao, F. Wang, and W. Mi, *J. Mol. Liq.* 219, 405 **(2016)**.
40. P. Pandey, A. K. Samanta, B. Bandyopadhyay, and T. Chakraborty, *J. Mol. Struct.* 975, 343 **(2010)**.
41. J. Depciuch, M. Sowa-Kućma, P. Misztak, B. Szewczyk, G. Nowak, P. Pankiewicz, and M. Parlińska-Wojtan, *Pharmacological Reports* **(2015)**.
42. B. Sarmento, D. Ferreira, F. Veiga, and A. Ribeiro, *Carbohydr. Polym.* 66, 1 **(2006)**.
43. I. M. Deygen and E. V. Kudryashova, *Colloids Surf., B: Biointerfaces* **(2016)**.
44. A. Kaler, R. Nankar, M. S. Bhattacharyya, and U. C. Banerjee, *J. Bionanosci.* 5, 53 **(2011)**.
45. E. Casals, T. Pfaller, A. Duschl, G. J. Oostingh, and V. Puntes, *ACS Nano* 4, 3623 **(2010)**.
46. M. R. Ivanov, H. R. Bednar, and A. J. Haes, *ACS Nano* 3, 386 **(2009)**.
47. S. H. Brewer, W. R. Glomm, M. C. Johnson, M. K. Knag, and S. Franzen, *Langmuir* 21, 9303 **(2005)**.
48. C. Zhou, M. Long, Y. Qin, X. Sun, and J. Zheng, *Angew. Chem.* 123, 3226 **(2011)**.
49. G. Dharanivasan, T. Rajamuthuramalingam, D. M. I. Jesse, N. Rajendiran, and K. Kathiravan, *Applied Nanoscience* 5, 39 **(2015)**.
50. J. A. Cowan, *Clin. Chem.* 49, 1565 **(2003)**.
51. R. M. Roat-Malone, Inorganic chemistry essentials, Bioinorganic Chemistry: A Short Course, 2nd edn., **(2007)**, pp. 1–28.
52. R. Sasikumar and R. Arunachalam, *Mater. Lett.* 63, 2426 **(2009)**.
53. A. Carré, W. Birch, and V. Lacarrière, *Silanes and Other Coupling Agents* 4, 1 **(2007)**.
54. B. Wang, Y. Chen, Y. Wu, B. Weng, Y. Liu, Z. Lu, C. M. Li, and C. Yu, *Biosens. Bioelectron.* 78, 23 **(2016)**.
55. P. Selvakannan, S. Mandal, S. Phadtare, A. Gole, R. Pasricha, S. Adyanthaya, and M. Sastry, *J. Colloid Interface Sci.* 269, 97 **(2004)**.
56. Y. Liu, J. Sun, J. Han, and Z. He, *Current Nanoscience* 6, 347 **(2010)**.
57. R. Yokel, E. Grulke, and R. MacPhail, *Wiley Interdisciplinary Reviews: Nanomedicine and Nanobiotechnology* 5, 346 **(2013)**.
58. R. Weissleder, M. Nahrendorf, and M. J. Pittet, *Nat. Mater.* 13, 125 **(2014)**.

Received: xx Xxxx xxxx; Accepted: xx Xxxxx xxxx